

Advanced Statistical Physics:

3. Frustration

Leticia F. Cugliandolo
leticia@lpthe.jussieu.fr

Sorbonne Université
Laboratoire de Physique Théorique et Hautes Energies
Institut Universitaire de France

Tuesday 26th November, 2019

Contents

3 Frustration	1
3.1 Definition and properties	1
3.1.1 The Ising model with nearest neighbour interactions	1
3.1.2 Antiferromagnetic models with continuous spins	4
3.1.3 Ising models with nearest and next-to-nearest competing interactions	5
3.1.4 General definition	5
3.2 Gauge invariance of Ising models	7
3.2.1 The Mattis model	7
3.2.2 Neural networks	7
3.3 Extensive entropy of the ground state	8
3.3.1 The Ising antiferromagnet on a triangular lattice	8
3.3.2 The fully frustrated model & the dimer models	11
3.3.3 The six vertex model	12
3.3.4 Other cases	16
3.4 Critical phases	16
3.5 The Coulomb frustrated Ising ferromagnet - periodic order	21
3.6 Order by disorder	25
3.6.1 The domino model	25
3.7 Discussion	28
3.A Some useful formulæ	29
3.A.1 Fourier transform	29
3.A.2 Stirling	30
3.A.3 Moments	30
3.A.4 Gaussian integrals	30
3.B Wick's theorem	32
3.C Functional analysis	33
3.D The saddle-point method	33

3 Frustration

In this Section we discuss the phenomenon of frustration and its main consequences. Frustration is the consequence of conflicting interactions. We focus on spin models.

Frustration makes the energy of the ground states be higher than the one of similar unfrustrated models. Moreover, frustration also enforces a large multiplicity of ground states, often associated with an *excess entropy* at zero temperature. We show how these two features arise in a number of celebrated statistical mechanics models. We also exhibit two other phenomena generated by frustration: the existence of *critical phases* and the one of *modulated phases*.

3.1 Definition and properties

A system is said to be frustrated [1] whenever it cannot minimise its total classical energy by minimising the energy of each group of interacting degrees of freedom. For two-body interactions, the minimisation should be done pair by pair but this is sometimes impossible, leading to frustration.

Frustration arises in many physical systems but it is most popular in the magnetic context, where the *geometry of the lattice* [2] and/or the *nature of the interactions* make the simultaneous minimisation of each term contributing to the energy impossible.

3.1.1 The Ising model with nearest neighbour interactions

We will now focus on Ising models, $s_i = \pm 1$, with nearest-neighbour interactions mediated by coupling strengths J_{ij} on a finite dimensional lattice

$$H_J[\{s_i\}] = -\frac{1}{2} \sum_{\langle ij \rangle} J_{ij} s_i s_j . \quad (3.1)$$

The sum runs over all pairs of nearest-neighbours on the lattice and the factor 1/2 ensures that each pair is counted only once.

For the Ising Hamiltonian (3.1) with generic J_{ij} (positive or negative) the minimum possible energy is obtained from the requirements

$$J_{ij} s_i s_j > 0 \quad \text{for all } ij \quad (3.2)$$

but it is not always possible to find a configuration that satisfies all these constraints.

Property 3.1 frustration Define the Ising model on a triangular lattice. Focus on one plaquette, as the ones shown in Fig. 3.1. Imagine that one exchange is negative, $J_{12} = -J$ and two are positive, $J_{23} = J_{13} = J$ with $J > 0$, all with the same magnitude. Taking

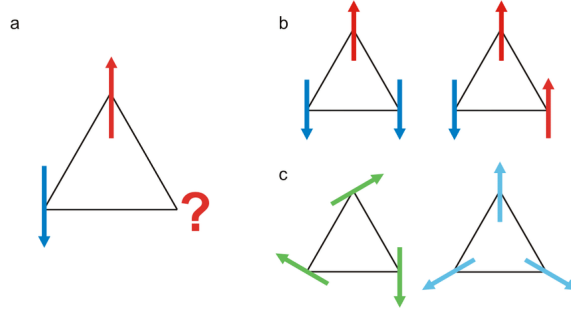


Figure 3.1: A plaquette of the triangular lattice. Panel (a) indicates that, for Ising spins, the third spin is frustrated and for any of the two possible orientations one link will yield a positive contribution to the energy. The two choices are shown in the upper figures in panel (b). Below, in (c), two configurations that minimise the energy of the single plaquette for XY spins coupled antiferromagnetically are shown. The angles between the spins are all equal to 120° . None of the single links are fully satisfied, that would have required anti-parallel spins.

into account the overall minus sign in Eq. (3.1), J_{12} favours anti-parallel alignment (antiferromagnetism, AF) while J_{13} and J_{23} favour the same orientation (ferromagnetism, FM). We list all possible spin configurations in Table 1, where we also give their energy and the name of the links that are *broken* or *unsatisfied*. There is no configuration with all links satisfied.

Property 3.2 energy spectrum The energy spectrum of the single triangular plaquette with $J_{12} = -J$ and $J_{23} = J_{13} = J$ is very simple. We add the contribution of each pair of spins only once. There are six degenerate ground states with energy $E_0 = -J$ and just two excited states with energy $E_1 = 3J$.

Property 3.3 degeneracy & entropy The six ground states are trivially divided in two classes related to each other by a global spin flip (1. and 8.; 2. and 7.; 3. and 6.). The two excited states (4. and 5.) are also related by the global reversal of all spins. The members of each pair of states share the same broken bond.

Property 3.4 excess energy & excess entropy Compared to a triangular plaquette with no frustration, that is to say, one in which all links have positive strength J , the ground state energy is increased by frustration. In the non-frustrated case $E_0 = -3J$ while in the frustrated case $E_0 = -J$. The ground state degeneracy is also increased by frustration. While in the non-frustrated case there are just two ground states related by symmetry, in the frustrated case there are six. One can pair these six states in groups of two *via* the reversal of all spins.

The property just described with an example can be generalised. We first note that $J_{12}J_{23}J_{13} < 0$ in the example. Take now the Ising model (3.1) with pairwise interactions on any lattice or graph. Any *loop of connected (nearest neighbours on the lattice or graph)*

#	s_1	s_2	s_3	E_{frust}	broken $_{\langle ij \rangle}^{\text{frust}}$	E_{FM}
1.	1	1	1	$-J$	12	$-3J$
2.	-1	1	1	$-J$	13	J
3.	1	-1	1	$-J$	23	J
4.	1	1	-1	$3J$	12, 23, 13	J
5.	-1	-1	1	$3J$	12, 23, 13	J
6.	-1	1	-1	$-J$	23	J
7.	1	-1	-1	$-J$	13	J
8.	-1	-1	-1	$-J$	12	$-3J$

Table 1: Ising spin configurations and their energy $E = -\sum_{\langle ij \rangle} J_{ij} s_i s_j$ (the contribution of each pair of spins is added only once) on a triangular plaquette. In the case named “frust” the exchanges are $J_{12} = -J$ (AF) and two positive, $J_{23} = J_{13} = J$ (FM) with $J > 0$. The next-to-last column names the link that is broken or unsatisfied. In the last column we add the energies of the same triangle in which all links favour ferromagnetic alignment.

Ising spins is frustrated if the product of the interaction strengths on the loop is negative,

$$\prod_{(ij) \in \text{loop}} J_{ij} < 0 \quad (3.3)$$

On such a loop, no choice of spin values minimises the contribution to the energy of *all* terms in the sum $\sum_{\langle ij \rangle} J_{ij} s_i s_j$.

In frustrated models such as the ones discussed up to now, in which all pairwise interactions have the same magnitude J , the ground state is the configuration that minimises the number of broken bonds or unsatisfied interactions.

Exercise 3.1 Take an antiferromagnetic Ising model on a square lattice in two dimensions. Is it frustrated?

Exercise 3.2 Take an Ising model on a square lattice in two dimensions and choose the couplings in such a way that (a) no plaquette is frustrated, (b) some plaquettes are frustrated, (c) all plaquettes are frustrated.

Exercise 3.3 Take the square plaquette in Fig. 3.2. A square plaquette with Ising spins placed on the vertices and nearest and next-nearest interactions with strengths J_1 and J_2 , respectively. Two Ising spins at the left-most sites, that we label s_1 and s_2 , are shown as an example. Other two Ising spins are placed on the upper right (s_3) and lower right (s_4) vertices. The plaquette’s energy is given by $H = -J_1(s_1 s_2 + s_2 s_3 + s_3 s_4 + s_1 s_4) - J_2(s_1 s_3 + s_2 s_4)$.

Give a condition on J_1 and J_2 so that the plaquette shown in Fig. 3.2 is not frustrated. Find its ground state configuration, and its energy and entropy for J_1 and J_2 satisfying this condition.

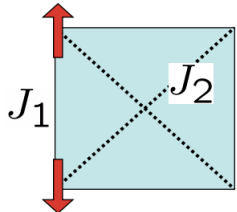


Figure 3.2: A square plaquette with Ising spins placed on the vertices and nearest and next-nearest interactions with strengths J_1 and J_2 , respectively. More details are given in the text.

Solution: The product of interactions on each triangular loop should be positive to avoid frustration. Therefore $J_1^2 J_2 > 0$ and this condition can be satisfied by either $J_1 > 0$ and $J_2 > 0$ or $J_1 < 0$ and $J_2 > 0$. In the former case the ground state configurations are such that $s_i = 1$ for all i or $s_i = -1$ for all i . The ground state energies and entropies of these FM states are $E_{\text{GS}}^{\text{FM}} = -4J_1 - 2J_2$ and $S_{\text{GS}}^{\text{FM}} = k_B \ln 2$. In the latter case, $J_1 < 0$ and $J_2 > 0$, antiferromagnetic ordering is favoured. The energies and entropies are $E_{\text{GS}}^{\text{AF}} = E_{\text{GS}}^{\text{FM}} = -4|J_1| - 2J_2$ and $S_{\text{GS}}^{\text{AF}} = S_{\text{GS}}^{\text{FM}} = k_B \ln 2$.

Consider now the choices of J_1 and J_2 so that the plaquette is frustrated and give its ground state configuration, energy and entropy.

Solution: There are again two choices such that $J_1^2 J_2 < 0$ to achieve frustration. (Note that the square loop is irrelevant in this respect, since $J_1^4 > 0$ for any choice of sign of J_1 .)

One choice is $J_1 > 0$ and $J_2 < 0$. If the ground state is FM, $s_i = 1$ for all i or $s_i = -1$ for all i , one has $E_{\text{GS}}^{\text{FM}} = -4J_1 + 2|J_2|$ and $S_{\text{GS}}^{\text{FM}} = k_B \ln 2$. If, instead, the ground state is two consecutive up spins and two consecutive down spins $E_{\text{GS}}^{2-2} = 0 - 2|J_2|$ and $S_{\text{GS}}^{2-2} = k_B \ln 4$. The FM configuration has lower energy iff $-4J_1 + 2|J_2| < -2|J_2| \Rightarrow J_1 > |J_2|$, otherwise the 2-2 configuration is the ground state.

If, instead, $J_1 < 0$ and $J_2 > 0$ and we focus on full AF ordering, $E_{\text{GS}}^{\text{AF}} = E_{\text{GS}}^{\text{FM}} = -4|J_1| + 2J_2$ and $S_{\text{GS}}^{\text{AF}} = S_{\text{GS}}^{\text{FM}} = k_B \ln 2$. There is no other competing candidate for a ground state in this case.

We end this part with the following conclusion: the existence of frustration depends on the lattice geometry and the interactions. For example, the Ising AF model in which all exchanges are $J_{ij} < 0$ is not frustrated on the $2d$ square lattice but it is on the triangular lattice. Indeed, for *bipartite lattices* such that each spin of one sublattice is only coupled to spins on the other sublattice, and the square lattice is one of these cases, the energy of the Ising model is simply minimised by the *Néel configuration* of alternating spins, in which the spins of one sublattice are parallel to each other and antiparallel to all spins of the other sublattice.

3.1.2 Antiferromagnetic models with continuous spins

Frustration also depends on the dimension of the variables; indeed, one could say that the “amount” of frustration depends on the type of spin variables. For instance, the XY AF, $H_J[\{\vec{s}_i\}] = -J \sum_{\langle ij \rangle} \vec{s}_i \cdot \vec{s}_j$, $J < 0$, and spins with two components, on the triangular lattice is “less frustrated” than the Ising one. The energy of an equilateral triangular

plaquette is minimised by a configuration with the spins pointing in directions at 120° , see Fig. 3.1 (c), and it equals $E_0 = 3J \cos 120^\circ = -3/2 J$, to be compared to $-3J$ in the ferromagnetic ground state (while for Ising spins the frustrated and non-frustrated plaquettes had ground state energies $-J$ and $-3J$). We are using a two-body Hamiltonian with no factor $1/2$ in front of it but we are counting the contribution of each pair of spins only once.

A necessity to satisfy the general condition of geometrical frustration with only antiferromagnetic exchange interactions is to have loops of odd length. Depending on the definition that we give to frustration, this is however not sufficient. For example, it is possible to minimise the energy of the classical antiferromagnetic Heisenberg model (spins with three components), $H_J[\{\vec{s}_i\}] = -J \sum_{\langle ij \rangle} \vec{s}_i \cdot \vec{s}_j$, and $J < 0$, on the triangular lattice with a simple helical arrangement of spins, and this defines a *unique* ground state. Then, the system is strictly speaking not geometrically frustrated. We associate *geometrical frustration* to the impossibility of finding a unique way (eliminating obvious symmetries) to minimise the energy.

With these example at hand, one can also relate the origin of frustration as *constraints*, or the impossibility of the microscopic variables to take all their possible values. The Ising spins are more constrained than the XY ones, since they cannot rotate on the plane but just take only two orientations.

3.1.3 Ising models with nearest and next-to-nearest competing interactions

Other examples of systems with frustration are those in which there are two (or more) kinds of *conflicting interactions* and not all can be satisfied simultaneously. Take for example the case of an Ising chain with nearest neighbour (nn) ferromagnetic and next nearest neighbour (nnn) antiferromagnetic interactions. Say that the strength of the former is J_1 and the one of the latter is J_2 . As long as $|J_2| \ll J_1$ the ground state is ferromagnetic: every nn bond is satisfied but the nnn ones are not. When $|J_2|$ exceeds a critical value, the ferromagnetic configurations are no longer the ground state. In both cases, both the nn and nnn bonds are not fully satisfied and the model is frustrated.

3.1.4 General definition

In the above examples the interaction between two spins was taken to be the usual one, $-Js_i s_j$. However, the concept of frustration can be applied to other kinds of variables (not only Ising) and other types of interactions as well, e.g. the Dzyaloshinski-Moriya interaction $-J|\vec{s}_i \wedge \vec{s}_j|$. A more general definition of frustration is the one that states that

a spin system is frustrated whenever the minimum of the system energy does not correspond to the minimum of all local interactions, whatever the form of the interactions.

The examples that we discussed above show that frustration depends on

- The geometry of the lattice.
- The interactions.
- The dimension of the variables.

Many interesting classes of classical and quantum magnetic systems are highly frustrated. This is the field of *constrained magnetism* [3, 4, 5] which is very active at present.

Anti-ferromagnets on a planar triangular lattice, spin-ice samples, the fully frustrated model and an Ising ferromagnet frustrated by Coulomb interactions are frustrated magnetic materials that we discuss below.

Exercise 3.5 Take an Ising model defined on a ring and with Hamiltonian

$$H = -\frac{K}{2} \sum_i (s_i s_{i+1} - 1) + \frac{J}{2} \left(\sum_i s_i \right)^2. \quad (3.4)$$

The coupling constants are $K > 0$ and $J > 0$.

1. How should the coupling constant scale with system size to have a reasonable competition between the two terms in H ?
2. How would you reduce the calculation of the partition function of this problem to the one of an Ising model with nearest-interactions on the same ring?
3. The phase diagram in the canonical and microcanonical ensemble are given in Fig. 3.3. What do you think the various line represent? Discuss the phase diagram in the context of the effects of long-range interactions and the inequivalence of ensemble discussed the first Chapter of these Lecures.

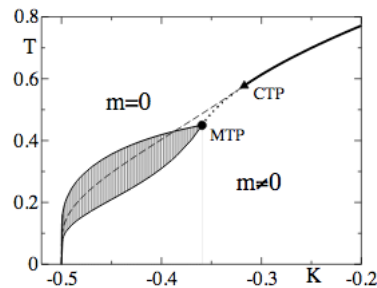


Figure 3.3: The phase diagram of the model defined in Eq. (3.4) and studied in Refs. [18]. The figure is taken from Ref. [19].

3.2 Gauge invariance of Ising models

The *gauge* transformation

$$\sigma_i = \epsilon_i s_i, \quad J'_{ij} = \epsilon_i J_{ij} \epsilon_j, \quad \text{with} \quad \epsilon_i = \pm 1 \quad (3.5)$$

leaves the energy and the partition function of an Ising spin model with two-body interactions invariant:

$$H_J[\{s_i\}] = H_{J'}[\{\sigma_i\}] \quad Z_J = Z_{J'}. \quad (3.6)$$

This invariance means that all thermodynamic quantities are independent of the particular choice of the interactions.

3.2.1 The Mattis model

Whenever it exists a set of ϵ_i s such that frustration can be eliminated from all loops in the model, the effects of quenched disorder are less strong than in truly frustrated cases. This is the case, for example, of the *Mattis model* [6]:

$$H_{\text{Mattis}} = - \sum_{ij} J_{ij} s_i s_j \quad \text{with} \quad J_{ij} = J(|\vec{r}_{ij}|) \xi_i \xi_j, \quad (3.7)$$

$J(|\vec{r}_{ij}|) > 0$, and the ξ_i taken from a probability distribution with a bimodal form, such that $\xi_i = \pm 1$. It is straightforward to see that under the transformation to new Ising variables

$$\sigma_i = \xi_i s_i \quad \forall i, \quad (3.8)$$

the Hamiltonian (3.7) becomes

$$H_{\text{Mattis}} = - \sum_{ij} J(|\vec{r}_{ij}|) \sigma_i \sigma_j \quad (3.9)$$

and it is not frustrated. (Note that the partition sum runs, in both representations, over Ising variables, $s_i = \pm 1$ or $\sigma_i = \pm 1$.) The fact that the model was not frustrated initially either can be seen from the fact that $\prod_{ij} J_{ij} = \prod_{ij} \xi_i \xi_j > 0$ over any closed loop, since all factors ξ_i appear twice in the product.

3.2.2 Neural networks

A particular case of the Mattis model is the *Hopfield model* of neural networks [7, 8]. It is defined by $H_{\text{Hopfield}} = - \sum_{ij} J_{ij} s_i s_j$ with $s_i = \pm 1$ representing the activity of a neuron and J_{ij} the synapsis between neurons assumed to be symmetric. Memory is proposed to be encoded in the form of the interaction strengths, with the form

$$J_{ij} = \frac{1}{M} \sum_{\mu=1}^M \xi_i^\mu \xi_j^\mu \quad \xi_i^\mu = \pm 1 \quad (3.10)$$

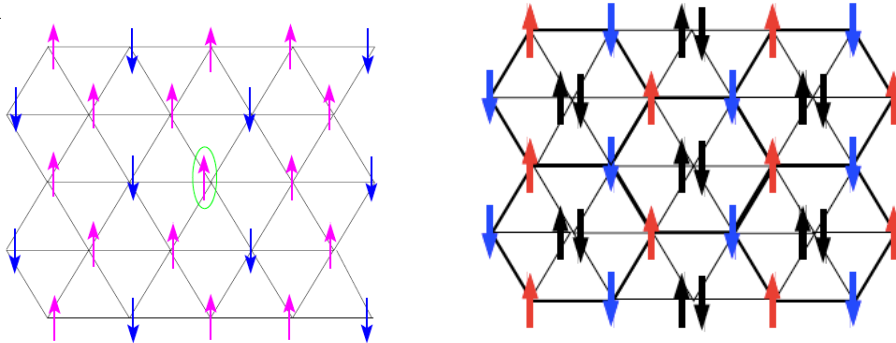


Figure 3.4: Left: the triangular lattice and a ground-state configuration. Each spin has six neighbours. The central one (surrounded in green) has zero local field $h_i^{\text{loc}} = \sum_{j(\text{nn}i)} s_j = 0$. Right: six triangles forming hexagons are singled out. The spins on the vertices of the hexagons are organised in perfect anti-ferromagnetic ordering but the inner spins are frustrated (figure taken from [5]).

and ξ_i^μ the *patterns* stored by the network.

Exercise 3.6 Study the Hopfield model defined on the complete graph, that is to say, when the sum runs over all pairs of spins in the sample, for a single pattern (a particular case of the Mattis model). For instance, find the neuronal configurations that minimise the energy.

3.3 Extensive entropy of the ground state

We show here how frustration enforces a large multiplicity of ground states, associated with a macroscopic *excess entropy* at zero temperature.

3.3.1 The Ising antiferromagnet on a triangular lattice

The model is defined as

$$H = -\frac{J}{2} \sum_{\langle ij \rangle} s_i s_j \quad (3.11)$$

with $s_i = \pm 1$, $J < 0$, and the sum running over first neighbours on the triangular lattice, see Fig. 3.4.

The minimal energy of any triangular plaquette, say E_0 , is reached by configurations such that there are two pairs of anti-parallel spins and one pair of parallel spins, $E_0^{\text{AF}} = -2J + J = -J$. A triangular plaquette with ferromagnetic interactions would have $E_0^{\text{FM}} = -3J$. An increment of $2J$ per plaquette is caused by frustration.

A lower bound

A lower bound for the $T = 0$ entropy is found recognising that

- The lattice can be thought of as the union of triangular plaquettes pointing up (we will ignore any possible finite size effect since we are interested in the thermodynamic limit).
- By simple inspection one can reckon that, in the thermodynamic limit, there are as many plaquettes pointing up as spins (again avoiding subtleties linked to boundary effects by taking $N \gg 1$):

$$\# \text{ spins} = \# \text{ up-plaquettes} = N . \quad (3.12)$$

- Joining six triangles one can construct an hexagon and see the triangular lattice as a centred honeycomb lattice (see the thick bonds in the right panel in Fig. 3.4).
- Therefore, there is one hexagon every three triangles pointing up and the number of hexagons is

$$\# \text{ hexagons} = \frac{N}{3} . \quad (3.13)$$

- On each hexagon one can arrange two configurations with perfect AF ordering.
- All the configurations of the kind shown in Fig. 3.4 are ground states. We can simply give a very rough lower bound to how many they could be. Let us take one of these configurations for the spins on the hexagons. There is a factor 2 due to the global spin reversal of the spins on the hexagons but this is irrelevant to the purposes to determining the leading order of the entropy we are looking for. The important one is the counting due to the freedom to choose the *orientation of the central spins* that leads to

$$\Omega_0^{\text{hex}} \propto 2^{N/3} . \quad (3.14)$$

- The actual entropy is therefore bounded from below by

$$S_0 \geq S_0^{\text{hex}} \approx \frac{k_B N}{3} \ln 2 \simeq 0.231 k_B N . \quad (3.15)$$

- Since we still have the liberty to choose the orientations of the spins on the hexagons in many ways (that could be exponential in N as well) the prefactor can change.

This argument already serves to prove that the entropy of the ground state is macroscopic, that is to say, proportional to N .

Pauling's argument

A slightly less crude counting of the number of ground states, Ω_0 , just considers the plaquettes as independent. The argument is originally due to Pauling to estimate the water ice zero-point entropy [9] and, for the AF model on the triangular lattice, goes as follows:

- The lattice can be thought of as the union of triangular plaquettes pointing up.
- By simple inspection one can first reckon that, in the thermodynamic limit, there are as many plaquettes pointing up as spins (we avoid subtleties linked to boundary effects by taking $N \gg 1$):

$$\# \text{ spins} = \# \text{ up-plaquettes} = N . \quad (3.16)$$

- The total number of (unconstrained) Ising spin configurations in a system with N spins is

$$(\# \text{ single spin configurations})^{\# \text{ spins}} = 2^N . \quad (3.17)$$

However, not all these configurations *are* energy minima.

- An approximation for the total number of configurations that are energy minima is given by the multiplication of this total number by a deflation weight factor equal to

$$\text{deflation weight per plaquette} = \left(\frac{\# \text{ ground states on a plaquette}}{\# \text{ states on a plaquette}} \right) \quad (3.18)$$

on each up-plaquette. This factor has to be taken to the power of the total number of up-plaquettes, which is equal to N the number of spins.

- This counting yields

$$\Omega_0 = (\# \text{ single spin conf.})^{\# \text{ spins}} \left(\frac{\# \text{ ground states on a plaquette}}{\# \text{ states on a plaquette}} \right)^{\# \text{ spins}}$$

Say there are N spins on the lattice. A plaquette has three spins and three pair interactions. The total number of configurations of the three Ising spins on a triangular plaquette is $2^3 = 8$. In the lowest energy configuration two pairs of spins are anti-parallel and one is parallel, see Fig. 3.4. The lowest energy configuration is obtained in six possible ways = 3 (which is the pair of anti-parallel spins) times 2 (global spin reversal). The fraction of minimal energy per all configurations of a plaquette is then $6/8$. Finally,

$$\Omega_0 = 2^N (6/8)^N \quad (3.19)$$

and the entropy of the ground states is

$$S_0 = k_B \ln \Omega_0 = k_B N \ln 3/2 \simeq 0.405 k_B N \quad (3.20)$$

and it is proportional to N . This argument overestimates by a little the entropy of the ground state, see eq. (3.21). One should have expected a large value of Ω_0 in this approximation since the plaquettes are taken to be independent and the fact that spins are shared by them is ignored.

Discussion

We are used to macroscopic entropies of $T \rightarrow \infty$ states but not to macroscopic entropies of ground states (recall the ferromagnetic Ising model with two ground states and $S_0 = k_B \ln 2$).

Such extensive residual zero temperature entropy is associated to a massive level of configurational spin disorder, that also gives rise to no phase transition down to zero temperature [10, 11]. As also said one classifies the frustration in this example as being geometric: it is the regular periodic structure of the (triangular) lattice that inhibits the long-range antiferromagnetic order.

The exact solution of this model was given by Wannier in the 50s [11], following the steps of Onsager's solution to the square lattice ferromagnetic model [12]. He obtained the residual entropy,

$$S_0 = 0.323 k_B N . \quad (3.21)$$

He also showed that there is no order at any finite temperature. It was proven later that the zero-temperature behaviour is “critical” in the sense that the correlation function decays algebraically, $C(r) \simeq r^{-1/2}$ [14]. We will come back to this property later.

Exercise 3.7 Take a square lattice in two dimensions and choose the couplings in such a way that all plaquettes are frustrated. Compare the minimal energy of the frustrated square plaquette to the one of an elementary unit with the same magnitude of coupling strengths but signs such that it is not frustrated. Compare also their entropy.

Exercise 3.8 Look at the simple arguments in [13] used to evaluate the zero-point entropy of an antiferromagnet in a magnetic field.

3.3.2 The fully frustrated model & the dimer models

The Hamiltonian is the Ising usual one

$$H_J[\{s_i\}] = -\frac{1}{2} \sum_{\langle ij \rangle} J_{ij} s_i s_j \quad (3.22)$$

with nearest neighbour interactions on the lattice. The exchanges J_{ij} have all the same modulus $|J_{ij}| = J$ and their product over ‘elementary polygons’ is negative. The elementary polygons are four-bond-squares for the square and simple cubic lattice, triangles for the FCC lattice, and hexagons for the diamond lattice [20]. By exploiting the transformation $\sigma_i = \epsilon_i s_i$ and $J'_{ij} = \epsilon_i \epsilon_j J_{ij}$ with $\epsilon_i = \pm 1$, the values of the new exchanges J'_{ij} can be rendered periodic. For a square lattice with periodic boundary conditions, there are many ways to achieve the latter. More precisely, there are four equivalence classes, corresponding to whether the product of the J s along a loop winding around a direction of the lattice is +1 or -1.

Exercise 3.9 Take the Ising model with nearest neighbour interactions on a square lattice in two dimensions. Take any realisation of J_{ij} s with the same magnitude such that the product of all the ones on each square plaquette equals -1 . Show that there is a choice of $\{\epsilon_i\}$ such that the interactions can be taken to be ferromagnetic on all rows, and ferromagnetic and anti-ferromagnetic on alternating columns.

As the interactions can be arranged regularly on the lattice, the free energy can be computed with standard methods. This model can be solved with the transfer matrix technique in $2d$. Villain showed that it has no thermodynamic instability at any finite T . However, the model is special at $T = 0$ as it has a high degeneracy of the ground state. The configurations of minimal energy have only one unsatisfied bond, such that $J'_{ij}\sigma_i\sigma_j < 0$. Each bond is shared by two plaquettes so the question of counting the number of ground states is equivalent to counting in how many ways one can place the *broken bonds* on the lattice with the constraint of having only one per plaquette. This is the so-called *dimer model* and its degeneracy was discussed in [27]. On the square lattice, $S_0 = k_B \ln \Omega_0 = k_B NC/\pi$ with C the Catalan number. The ground state energy is $E_0 = -NJ$ as exactly one quarter of the links are unsatisfied. In the thermodynamic limit, the low temperature expansion of the free-energy density reads

$$\beta f(\beta) = \beta e_0 - s_0 + c_1 \beta e^{-2\beta J} . \quad (3.23)$$

The equilibrium correlation length is expected to diverge as $\xi_{\text{eq}} \simeq e^{\beta J}$. The model has no long-range order of any kind, even at $T = 0$.

On other lattices, or for other kinds of spins, a finite temperature transition can be found.

These two examples showed that

phase transitions can be avoided due to frustration

3.3.3 The six vertex model

In vertex models the degrees of freedom (Ising spins, q -valued Potts variables, etc.) sit on the edges of a lattice. The interactions take place on the vertices and involve the spins of the neighbouring edges.

Take an $L \times L$ square lattice with periodic boundary conditions. Label the coordinates of the lattice sites (m, n) . This lattice is *bipartite*, namely, it can be partitioned in two sub-lattices A_1 and A_2 such that the sites with $m + n$ even belong to A_1 , those with $m + n$ odd belong to A_2 , and each edge connects a site in A_1 to one in A_2 . The degrees of freedom sit on the links between two sites or, in other words, on the “medial” lattice whose sites are placed on the midpoints of the links of the original lattice. The midpoints are hence labeled by $(m + 1/2, n)$ and $(m, n + 1/2)$. Thus, the degrees of freedom are

arrows aligned along the edges of a square lattice, which can be naturally mapped onto Ising spins, say $s_{m+1/2,n} = \pm 1$. Without loss of generality, we choose a convention such that $s = +1$ corresponds to an arrow pointing in the right or up direction, depending on the orientation of the link, and conversely $s = -1$ corresponds to arrows pointing down or left.

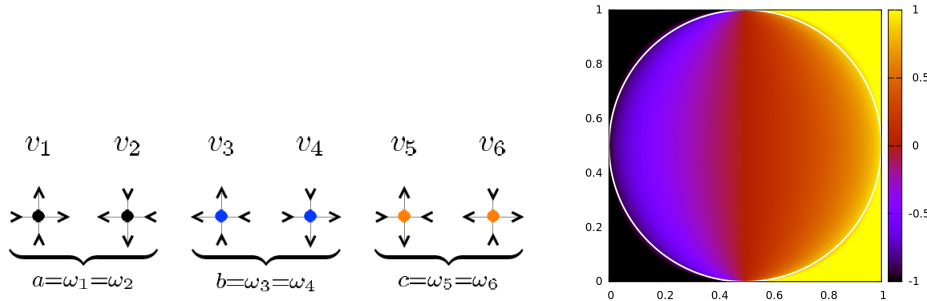


Figure 3.5: The six vertex configurations of the six vertex model and a configuration with the arctic curve [26].

In the six-vertex model (or $2d$ spin-ice) arrows (or Ising spins) are constrained to satisfy the two-in two-out rule. Each node on the lattice has four spins attached to it with two possible directions, as shown in Fig. 3.5.

The model was proposed to describe ferroelectric systems by giving different statistical weights to different vertices: $w_k \propto e^{-\beta \epsilon_k}$ with ϵ_k the energy of each of the $k = 1, \dots, 6$ vertices. $\beta = 1/(k_B T)$ is the inverse temperature. Spin reversal symmetry naturally imposes $w_1 = w_2 = a$ for the first pair of ferromagnetic (FM) vertices, $w_3 = w_4 = b$ for the second pair of FM vertices, and $w_5 = w_6 = c$ for the anti-ferromagnetic (AF) ones, see Fig. 3.5. We have here introduced the conventional names a , b , and c of the Boltzmann weights of the three kinds of vertices. It is customary to parametrize the phase diagram and equilibrium properties in terms of a/c and b/c , as shown in the phase diagram in Fig. 3.6. It is important to note, however, that in the context of experiments in artificial spin-ice type samples, vertex energies are fixed and the control parameter is the temperature.

The free-energy density of the model with periodic boundary conditions can be computed with the transfer matrix technique and the Bethe Ansatz to solve the eigenvalue problem [23, 24].

Excess ice entropy

Take the case $a = b = c$ in which all vertices are equivalent, the so-called spin-ice point. A simple counting argument was put forward by Pauling to estimate the number of configurations that satisfy the two-in two-out constraint [9]. It is very similar to the one already exposed for the planar antiferromagnet on the triangular lattice. Take a system with N vertices. On the square lattice each vertex has $z = 4$ neighbouring vertices

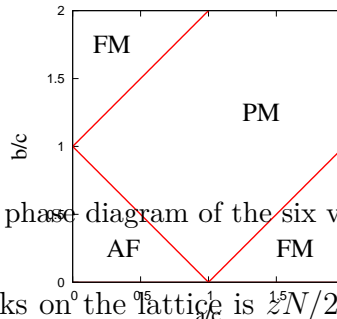


Figure 3.6: The phase diagram of the six vertex model.

attached to it. The number of links on the lattice is $zN/2^2$ as each link is shared by two vertices. In principle, each link can take two configurations for Ising spins, therefore, ignoring the constraint, there are $2^{zN/2}$ possible arrow configurations. The constraint definitely diminishes the number of allowed configurations but it cannot be taken into account exactly in this kind of simplified argument. Pauling's proposal was to consider it in a kind of *mean-field* way, by simply assuming that the number of configurations is reduced by a factor given by the ratio between the allowed vertex configurations and all vertex configurations ($6/16$) for each vertex. Finally,

$$\Omega_0 = 2^{zN/2} (6/16)^N \quad \Rightarrow \quad S_0 = k_B N \ln \frac{3}{2} \simeq 0.405 k_B N. \quad (3.24)$$

This result is very close to the numerical one $S_0 \simeq 0.410 k_B N$ [22]. The exact solution of Lieb yields $S_0 = -3/2 \ln 3/4 k_B N \simeq 0.431 k_B N$ [23, 24].

Exercise 3.10 Take a single vertex and compute the number of ground states Ω_0 exactly and with Pauling's argument. Take then two vertices and consider separately free (FBC) and periodic boundary conditions (PBC), compute $\Omega_0^{(\text{FBC})}$ and $\Omega_0^{(\text{PBC})}$ exactly, and compare these values to Pauling's estimate. Repeat for a square plaquette made of four vertices. Conclude.

A comparison between Pauling's estimate for the zero-point entropy and its actual measurement via

$$\Delta S = S(T_2) - S(T_1) = \int_{T_1}^{T_2} dT' \frac{C(T')}{T'} \quad (3.25)$$

in a spin-ice sample is shown in Fig. 3.7. One takes $T_2 \rightarrow \infty$ with $S(T_2) = k_B N \ln 2$. This is a magnetic material with a similar crystalline structure to the one of water ice, thus its name.

Phase diagram

The statistical properties of the model can be studied for generic values of the parameters a , b and c . A phase diagram with two FM ordered phases (large values of a or b with

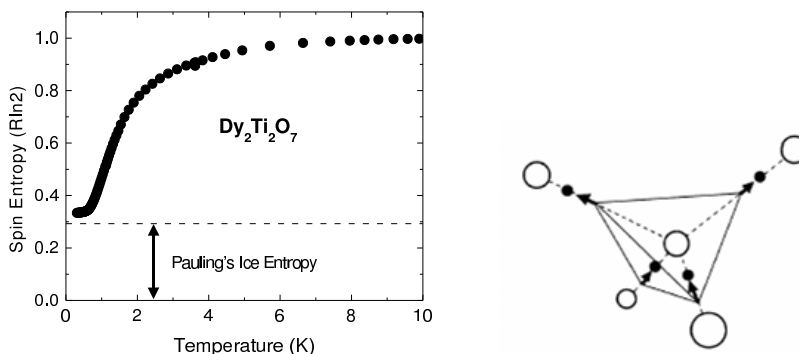


Figure 3.7: Left: Entropy of a spin-ice sample [25]. Right: the tetrahedra cell in water and spin ice. In the former case, the large open circles represent the O atoms and the small filled ones the H atoms. In the latter case, the arrows represent the moments of the magnetic atoms.

respect to c), one AF phase (large value of c) and one disordered phase (similar values of all the parameters) are found. The disordered phase is very peculiar as it is *critical* meaning that the spatial correlations decay algebraically with distance

$$C(r) \simeq r^{-\eta} \quad (3.26)$$

with the exponent η a function of the control parameters a/b and a/c . This is also called a Coulomb phase. We discuss critical phases in Sec. 3.4.

Boundary conditions and macroscopic phase separation

The effect of the boundary conditions is very subtle in these systems, as some thermodynamic properties depend upon them, in contrast to what happens in usual short-range statistical physics models. (These systems present macroscopic phase separation in real space. A frozen region fixed by the boundary conditions is separated from a fluctuating phase by the so-called *arctic curve*. A similar phenomenon exists in crystal growth [21].)

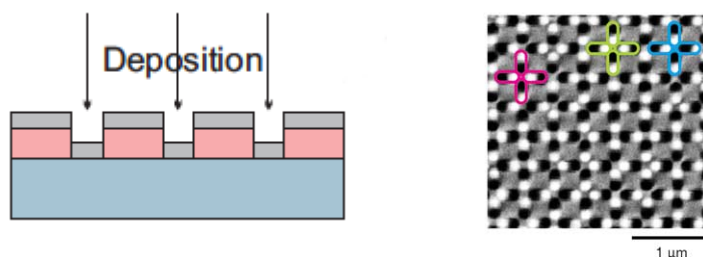


Figure 3.8: Left: Sketch of artificial spin-ice preparation. Right: A typical configuration.

These examples showed the phenomenon

Fluctuations \mapsto degeneracies \mapsto zero-point entropy

This result seems to violate the third law of thermodynamics, that states $S(T \rightarrow 0) = 0$. This is however not so, as quantum fluctuations will come to help at sufficiently low temperatures and re-establish this limit.

3.3.4 Other cases

Up to now we have studied models with the same exchange coupling magnitude. What happens if we allow for exchanges taking different real values? We explore this case with an example.

Exercise 3.11 An Ising spin model with $N = 5$ spins and two body interactions J_{ij} is defined on a random graph. The exchanges

$$\begin{array}{lll} J_{12} = -1.00 & J_{25} = 0.4 & J_{23} = -0.1 \\ J_{35} = 0.81 & J_{34} = -0.7 & J_{45} = 0.03 \end{array}$$

couple the spins labeled with i and j .

1. Give a schematic representation of this system.
2. Is it frustrated? Justify the answer.
3. We will call this system A. Take now another system, that we will call B, in which all the interactions are ferromagnetic, with the same absolute values. Which ground state energy is lower, the one of A or the one of B?
4. Which ground state entropy is lower?
5. Are the results of questions (3) and (4) generic? Why?

3.4 Critical phases

The zero temperature statistical average of any observable involves an averaging over all ground states. In cases in which the ground state is infinitely degenerate, this implies an average over an infinite number of states. In particular, correlations should be computed in this way. Naively, one could imagine that averaging over an infinite number of different states will generally lead to effective disorder and the impossibility of having any kind of order. However, this is not always the case and most systems that have an infinite but discrete ground-state degeneracy turn out to exhibit *algebraic correlations* and hence *quasi-long-range order*.

The spin-spin correlation function in the AF Ising model on the triangular lattice decays as

$$C(r) \equiv \langle s_i s_j \rangle_{|\vec{r}_i - \vec{r}_j| = r} \simeq r^{-1/2} . \quad (3.27)$$

The original proof by Stephenson is too involved to be reproduced here [14]. We will present, instead, an argument that is quite commonly used in this kind of problems and that is based on a beautiful mapping onto a *height model* [15, 17]. Such models represent the spin fluctuations by assigning to each point a height h_i and are usually called *solid-on-solid* models. They describe the *roughening transition* between a flat surface, where the height displacement, typically measured by $\langle (h_i - h_j)^2 \rangle$, is bounded from above, and a rough surface, where the height differences diverge.

First of all, let us define the concept of *dual lattice*. For any planar network of bonds, one can define a geometrical dual by connecting the centres of neighbouring plaquettes. Each bond of the dual lattice crosses a bond of the original lattice. The mapping taking from the original to the dual lattice is therefore local. Clearly, the dual of a triangular lattice is a hexagonal (or honeycomb) lattice, and vice versa.

The mapping onto height variables proceeds as follows.

- Take a ground state of the original triangular lattice and identify all the broken links (one per plaquette).
- To each ground state of the Ising model, one associates a dimer covering of the dual honeycomb lattice, putting a dimer on each bond that crosses a broken link (spins aligned FM) of the original triangular lattice, see the thick black dimers in Fig. 3.9.
- One associates a direction to each bond of the triangular lattice in such a way that there is, say, clockwise circulation around up-pointing triangles and anti-clockwise circulation around down-pointing triangles.
- The (microscopic) height variables h_i , taking integer values are defined on the vertices of the original triangle lattice, as shown in red in Fig. 3.9.
- After choosing the height of one reference site (which one it is, is arbitrary) one associates to each dimer covering a height configuration following the prescription that, when going clockwise around an up triangle, the height *difference* between neighbouring sites is equal to 2 if one crosses a dimer and -1 if one does not cross a dimer. With this prescription, the height differences around all triangles (up and down) is zero, ensuring that the height variable is single valued, and the assignment is consistent. (Another possible prescription would be the one in which we assign -2 and 1 , to the two cases, respectively.)

The ground state condition in the spin model translates into the single valued-ness of the height variable. Accordingly, the height configuration does not depend on the path chosen for its construction.

The height differences between neighbouring sites do not exceed 2. One can see that the height configurations are such that the lattice is divided in three sub-lattices and on each of them the height variables, defined modulo 3, $\bar{h}_i = h_i \pmod{3}$, take values 0, 1, 2. It is clear that, as the total magnetisation density of the ground states vanishes, $m = N^{-1} \sum_i s_i = 0$, there should be as many 0s plus 2s, as there are 1s in the height configuration defined modulo 3.

Conversely, from each solid-on-solid (SOS) configuration subject to these restrictions, one can obtain a spin configuration by requiring that odd and even height variables

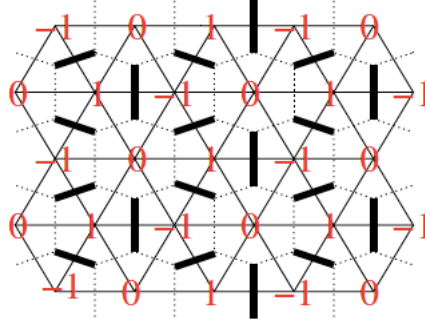


Figure 3.9: A ground state configuration of the AF model on the triangular lattice. The dimer covering on its dual honeycomb lattice in which each thick bond crosses a broken link. The height assignment is represented by the integers in red. The image is copied from [5].

conf	s_1	h_1	s_2	h_2	s_3	h_3	$h(\vec{r})$
1	1	h	2	$h + 1$	3	$h - 1$	h
2	1	h	2	$h - 2$	3	$h - 1$	$h - 1$
3	1	h	2	$h + 1$	3	$h + 2$	$h + 1$

Table 2: Table with the spin and height values in an up-looking plaquette for which the left-most spin has been fixed to $s_1 = 1$ and its height value to $h_1 = h$.

correspond to spins of different sign; more precisely

$$s_i = \begin{cases} 1 & \text{if } h_i \text{ even} \\ -1 & \text{if } h_i \text{ odd} \end{cases} \quad (3.28)$$

Next, instead of working with the h_i discrete variables, *via* a coarse-graining one defines new height variables

$$h(\vec{r}) = [h_i + h_j + h_k]/3, \quad (3.29)$$

where i, j, k are the sites that belong to the same triangle and $\vec{r} = [\vec{r}_i + \vec{r}_j + \vec{r}_k]/3$ is a site on the dual lattice, that is to say, at the centre of the triangles. The coarse-grained heights are therefore defined on the hexagonal lattice.

As an example take an up-looking triangle, start from the left-most vertex and locate a spin up $s_1 = 1$ on it, call its reference height $h_1 = h$. The three possible ground state configurations, the local height variables and the central coarse-grained one are given in Table 2. While the site heights can vary at most by two units, and take values $h - 2, h - 1, h, h + 1, h + 2$, the central coarse-grained height can vary only by one unit and takes values $h - 1, h, h + 1$.

Two spin configurations around an hexagon and at its center are shown in Fig. 3.10, that is taken from [17]:

- The configuration in the left panel is one of the ones used to obtain the lower bound for the ground state entropy. It has AF order around the hexagon and a flippable spin (at no energetic cost) at the center. The height configuration on the triangular lattice sites is almost flat, with height differences equal to ± 1 at most. The coarse-grained height configuration is completely flat, with $h(\vec{r}) = h$ on the six triangles.
- The configuration in the right panel is also a ground state, as each triangle has only one broken link. However, one can check that flipping any spin the energy increases. Take, for instance, the spin lying at the left-most end. If it flips from down to up, two links break and only one heals leading to an increase in the global energy. The same applies to all other spins in the group. The height configuration on the triangular lattice sites is rougher in this case and the coarse-graining does not completely erase the fluctuations.

The flat surface corresponds to $h(\vec{r}) = h$ everywhere and it is supposed to be the one with maximal statistical weight. Therefore, one proposes the *entropic probability density*

$$P[\{h\}] = \mathcal{Z}^{-1} e^{\frac{K}{2} \int d^2r |\vec{\nabla} h(r)|^2} = \mathcal{Z}^{-1} e^{-\frac{K}{2} \sum_{\vec{q}} q^2 |h(\vec{q})|^2} \quad (3.30)$$

with K some effective coupling, supposedly proportional to J . From here one computes the average of any mode

$$\langle |h(\vec{q})|^2 \rangle = \frac{\int dh h^2 e^{-\frac{K}{2} q^2 h^2}}{\int dh e^{-\frac{K}{2} q^2 h^2}} = \frac{1}{K q^2} \quad (3.31)$$

which implies

$$\langle [h(\vec{r}) - h(\vec{0})]^2 \rangle \propto \sum_{\vec{q}} (1 - e^{i\vec{q}\cdot\vec{r}}) \frac{1}{K q^2} \propto \frac{1}{2K} \ln \frac{\pi r}{a} \quad (3.32)$$

for large r , with a a short distance cut-off (the lattice spacing). *Recall the calculation of the angle correlations in the spin-wave approximation of the 2d XY model.* From the point of view of the roughness properties of the manifold $h(\vec{r})$, it is in its *rough phase*, since the mean-square displacement diverges logarithmically.

To extract the correlations of the Ising model, one must relate the spin variables s_i to the height variables h_i . This relation is not simple, but it is enough to realise that the spin variables have to be periodic functions of the height variables of period six. Indeed, turning the spins around a triangle twice leads to the same configuration, while the height has changed by 6. So any local operator of the spin $O(s)$ can be expanded as

$$O(\vec{r}) = \sum_{n=1}^{\infty} O_n e^{i\frac{2\pi n}{6} h(\vec{r})} \quad (3.33)$$

Let us evaluate the behaviour of the correlation between any two such terms. Using the identity for Gaussian fields, and the result (3.32) for the height displacement, the

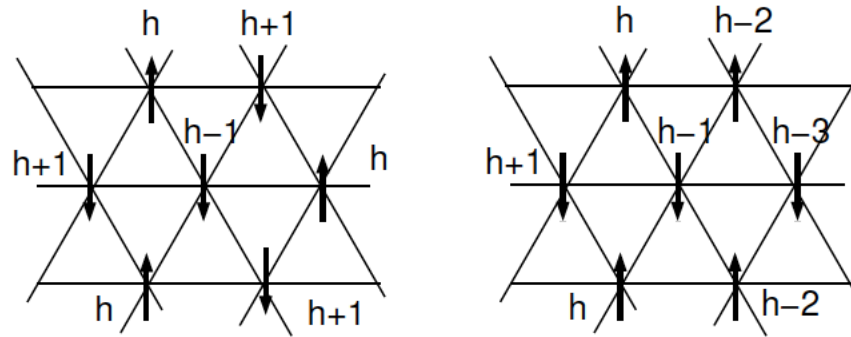


Fig. 1.6 Triangular lattice Ising antiferromagnet spin configurations and mappings to height field. Left: state with flippable spin generating a flat height field (with the value h at all triangle centres). Right: spin state without flippable spins, that generates a height field with maximum gradient (heights at triangle centres decrease by 1 on going from any triangle to its right-hand neighbour).

Figure 3.10: Image taken from [17]. See the text for a discussion.

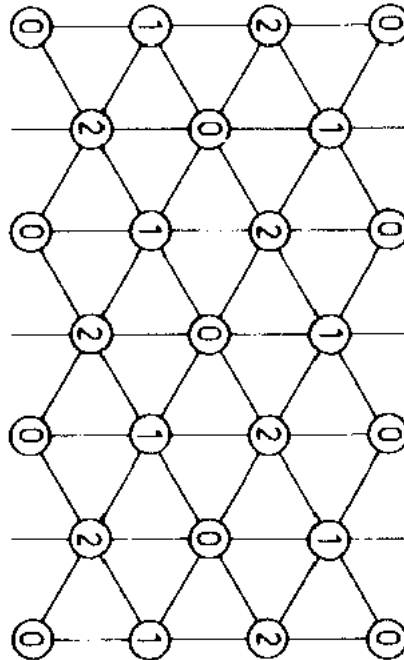


Figure 3.11: Image taken from [16]. See the text for a discussion.

self-correlation of any of the terms in (3.33) reads

$$\begin{aligned} \left\langle \exp \left\{ -i \frac{2\pi n}{6} [h(\vec{r}) - h(\vec{0})] \right\} \right\rangle &= \exp \left\{ -\frac{\pi n}{6} \langle [h(\vec{r}) - h(\vec{0})]^2 \rangle \right\} \\ &\simeq \exp \left[-\frac{\pi n}{6} \frac{1}{2K} \ln \left(\frac{\pi r}{a} \right) \right] \end{aligned} \quad (3.34)$$

it is clear that for large r the contribution of the smallest n value to the sum will be the most relevant one (this also justifies having studied the self-correlation). Thus one takes

$$s(\vec{r}) \propto e^{i \frac{2\pi}{6} h(\vec{r})} \quad (3.35)$$

to calculate the spin-spin correlation of spins on the same sublattice (so that alignment between them is expected and thus avoid including signs to capture the staggered AF order)

$$\langle s(\vec{r}) s(\vec{0}) \rangle \propto \left(\frac{\pi r}{a} \right)^{-\eta} \quad \eta = \frac{\pi}{18K}. \quad (3.36)$$

The power-law form illustrates the consequences of large but strongly correlated ground state fluctuations. Comparing this result with the exact result that the correlations decay as $r^{-1/2}$ one concludes that the value $K = \pi/9$ has to be chosen to match it.

The main approximation that has been made in using the height model to represent the triangular lattice Ising AF is to treat $h(\vec{r})$ as a real, rather than integer-valued field. This fact can be taken into account by adding a term to the Hamiltonian that favours integer h values. The RG analysis shows that this term is irrelevant for $K < \pi/2$. Since the value of K that corresponds to the Ising AF is $K = \pi/9$, one concludes that the results found with the real approximation are correct.

The results discussed above are reminiscent of the ones that we derived for the low-temperature phase of the $2d$ XY model, in the spin-wave approximation. The similarity can be taken further. Excitations out of the ground state have a simple description in the height-model language. If the three Ising spins of an elementary triangle have the same orientation, the height field is no longer everywhere single-valued: it changes by $+6$ on encircling the triangle that carries the excitation. A single spin flip can introduce such excitations into a ground-state configuration only as a vortex anti-vortex pair that can be separated by additional spin flips without further increase in exchange energy.

3.5 The Coulomb frustrated Ising ferromagnet - periodic order

In many systems a short-range tendency to order is opposed by a long-range force that frustrates this order. The low-temperature phase of these systems is characterised by stripe of checkerboard order. A model in this class is an Ising ferromagnet with short-range exchanges frustrated by antiferromagnetic Coulomb interactions. More precisely,

the model is described by the Hamiltonian [28]

$$H_{J,Q}[\{s_i\}] = -\frac{J}{2} \sum_{\langle ij \rangle} s_i s_j + \frac{Q}{2} \sum_{i \neq j} v(\vec{r}_{ij}) s_i s_j, \quad (3.37)$$

where, $J, Q > 0$ are the ferromagnetic and antiferromagnetic coupling strengths between the Ising spin variables $s_i = \pm 1$ placed on the sites of a three-dimensional cubic lattice. The first sum is restricted to nearest neighbours (each pair is added twice) while the second one runs over all pairs of spins on the lattice. \vec{r}_{ij} is the vector joining sites i and j , and $v(\vec{r})$ is a Coulomb-like interaction term with $v(\vec{r}) \sim 1/|\vec{r}|$ for $|\vec{r}| \rightarrow \infty$.

Because of the Coulomb interaction, the existence of the thermodynamic limit requires that the total magnetization of the system be zero. As a consequence, the ferromagnetic order is forbidden at all temperatures and for any nonzero value of the frustration parameter Q/J . In three dimensions, the system has an order-disorder transition at finite temperature with a complex frustration-temperature phase diagram with a variety of *modulated phases*.

The Hamiltonian (3.37) is quadratic in the spin variables. The interactions are not local in real space but they depend only on the distance between the two spins involved in each term. H can be written as

$$H_{J,Q}[\{s_i\}] = - \sum_{i \neq j} V(\vec{r}_{ij}) s_i s_j \quad \text{with} \quad V(\vec{r}_{ij}) = \frac{J}{2} \delta(\vec{r}_{ij}, a \hat{e}_{ij}) - \frac{Q}{2} v(\vec{r}_{ij}), \quad (3.38)$$

a the lattice spacing, \hat{e}_{ij} the unit vector linking the site i to the site j and $\delta(x, y)$ the Kronecker delta-function. It is then convenient to diagonalise the Hamiltonian by going to Fourier space

$$H_{J,Q}[\{s_i\}] = \frac{J}{2} \sum_{\vec{k}} \hat{V}(\vec{k}) |\hat{s}(\vec{k})|^2 \quad (3.39)$$

where $\hat{s}(\vec{k})$ is the lattice Fourier transform of the Ising spin variables s_i placed on the lattice, see App. 3.A.1. It is computationally convenient to choose the Fourier representation of the Coulomb-like interaction to be

$$v_A(\vec{r}) = \frac{4\pi}{N} \sum_{\vec{k}} \frac{\exp(-i\vec{k}\vec{r})}{2 \sum_{\alpha=x,y,z} (1 - \cos k_\alpha)}, \quad (3.40)$$

where N is the number of lattice sites and the sum over $\vec{k} = (k_x, k_y, k_z)$ is restricted to the first Brillouin zone. This form approaches $1/r$ at large r and deviates from the Coulomb law at $r \simeq 0$. In particular, $v_A(r=0) \neq 0$. The Fourier transform of the interaction potential takes a simple form

$$\hat{V}(\vec{k}) = -2 \sum_{\alpha=x,y,z} \cos k_\alpha + \frac{4\pi Q}{J} \left[\frac{1}{2 \sum_{\alpha=x,y,z} (1 - \cos k_\alpha)} - v_A(\vec{r} = \vec{0}) \right] \quad (3.41)$$

where the subtraction of $v_A(\vec{r} = \vec{0})$ serves to cure any problems at $\vec{r} = \vec{0}$, see [28] for more details. Note that in the continuous limit ($\vec{k} \rightarrow \vec{0}$) the familiar k^2 harmonic form is recovered in the first term and the second term goes as $1/k^2$.

For $Q = 0$ the model reduces to the standard Ising ferromagnet, and the ground state is ferromagnetically ordered. Oppositely, for $J = 0$ the model is equivalent to a Coulomb lattice gas (with the mapping between spin and occupation number variables, $n_i = (1 - s_i)/2$) and the ground-state is a Néel antiferromagnetic state. When $Q \neq 0$, the Coulomb interaction prevents the existence of a ferromagnetic phase, and in the thermodynamic limit, the total magnetisation (charge) is constrained to be zero. Instead, phases with modulated order, with periodic patterns of “up” and “down” spins subject to the constraint of zero magnetisation, are formed.

Mean-field approximation

In order to describe phases with spatial modulation one needs to keep the local character of the local magnetisation at site i , $m_i = \langle s_i \rangle$, in the mean-field approximation discussed in the chapter on phase transitions. The free-energy density is

$$f(\{m_i\}) = -J \sum_{i \neq j} V(r_{ij}) m_i m_j - \sum_i \left[\frac{1 + m_i}{2} \ln \frac{1 + m_i}{2} + \frac{1 - m_i}{2} \ln \frac{1 - m_i}{2} \right]. \quad (3.42)$$

The local mean-field equations read

$$m_i = \tanh(\beta H_i) \quad \text{with} \quad H_i = -J \sum_{j(\neq i)} V_{ij} m_j \quad (3.43)$$

the effective field on site i . In the case $Q = 0$, $H_i = -J \sum_{j(\text{nn}i)} m_j - h_i$ with h_i an external local magnetic field, if there is one and one recovers the well-known Curie-Weiss approximation.

Close to a second-order phase transition the magnetisations are expected to be small and (3.43) can be linearised,

$$m_i \approx \beta H_i \quad \Rightarrow \quad \hat{m}(\vec{k}) \approx \beta \hat{H}(\vec{k}) \quad \text{and} \quad H(\vec{k}) = -J \hat{V}(\vec{k}) \hat{m}(\vec{k}). \quad (3.44)$$

This equation has two kinds of solutions. The paramagnetic one, $\hat{m}(\vec{k}) = 0$ for all \vec{k} and non-trivial ones, $\hat{m}(\vec{k}) \neq 0$, at least for some \vec{k} . The former one is the high-temperature solution, and the latter appear at the critical temperature $T_c(J, Q)$.

For a given value of the frustration parameter, Q , the critical temperature $T_c(J, Q)$ is then given by

$$T_c(J, Q) = -J \min_{\vec{k}} \hat{V}(\vec{k}) \equiv -J V_c(Q/J), \quad (3.45)$$

where the minimum of $\hat{V}(\vec{k})$, $V_c(Q/J)$, is attained for a set of nonzero wave-vectors $\{\vec{k}_c(Q/J)\}$ that characterise the ordering at $T_c(J, Q)$.

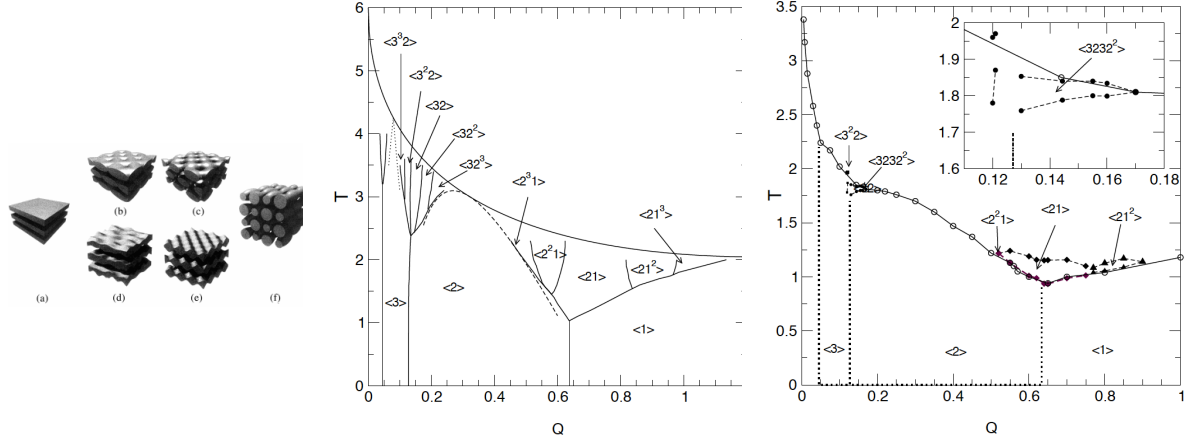


Figure 3.12: Examples of lamellar (a), (b) and (d) and columnar (c) order in block-polymer systems [29]. The mean-field and Monte Carlo phase diagrams of the model discussed in this Section [28] (note the different normalisation, factor 2 between the two phase diagrams).

For the inverse lattice Laplacian expression of the long-range frustrating interaction in $d = 3$, eq. (3.41), the $\vec{k}_c(Q/J)$'s vary continuously with Q/J :

$$\begin{aligned}
 \vec{k}_c &= (\pm \arccos(1 - \sqrt{\pi Q/J}), 0, 0) & \text{for } 0 \leq Q/J < 4/\pi \\
 \vec{k}_c &= (\pi, \pm \arccos(3 - \sqrt{\pi Q/J}), 0) & \text{for } 4/\pi \leq Q/J < 16/\pi \\
 \vec{k}_c &= (\pi, \pi, \pm \arccos(5 - \sqrt{\pi Q/J})) & \text{for } 16/\pi \leq Q/J < 36/\pi \\
 \vec{k}_c &= (\pi, \pi, \pi) & \text{for } 36/\pi \leq Q/J
 \end{aligned} \tag{3.46}$$

and all permutations of the x, y, z coordinates in Eqs. (3.46). The above ordering wavevectors correspond, respectively, to lamellar (full FM order in two directions, for small Coulomb AF frustration), tubular (full FM order in only one direction, for slightly larger Coulomb AF frustration), orthorhombic, and cubic or Néel (for still large AF long-range frustration) phases, see Fig. 3.12. The corresponding critical temperature $T_c(Q)/J$ are then given by

$$T_c(Q/J) = J \left(6 - 4\sqrt{\pi Q/J} + 4\pi Q v(0) \right) \quad \text{for } 0 \leq Q/J \leq 36/\pi \tag{3.47}$$

$$T_c(Q/J) = J (-6 + 4\pi Q/J (v(0) - 1/12)) \quad \text{for } 36/\pi \leq Q/J \tag{3.48}$$

The mean-field approximation gives a line of second-order phase transitions from the disordered to the modulated phases. For vanishing small frustrations, the critical temperature goes continuously to T_c^0 , the critical temperature of the pure Ising ferromagnet. More details on this problem can be found in [28].

The mean-field analysis of this model showed the existence of a complex phase diagram and very different kinds of order depending on the coupling strengths J and Q and their relative value. The effect of the frustration exhibited in this model can be summarised as

Frustration \mapsto complex phase diagram with fancy phases

3.6 Order by disorder

Fluctuations tend to disorder typical systems. However, in a class of magnetic systems order is induced by fluctuations, be them thermal or quantum. The *order by disorder* phenomenon was introduced in [33] and discussed in general in [34]. It arises in systems with infinitely degenerate rather than unique classical ground state. This property can be due to the spatial geometry of the lattice, or the peculiar organisation of the coupling strengths and it is intimately related to frustration. The principal effect of frustration is to ensure that the classical ground state manifold is of higher symmetry than the underlying Hamiltonian. Quantum or thermal fluctuations can dynamically break this additional symmetry, restoring that of the Hamiltonian.

3.6.1 The domino model

The domino model is an Ising model on a rectangular lattice with two kinds of atoms placed along alternating columns and nearest-neighbour interactions. The tree interaction strengths are: $J_{AA} > 0$ between nearest-neighbour A atoms on a vertical A column, $J_{BB} < 0$ between nearest-neighbour B atoms on a vertical B column, and $J_{AB} > 0$ between nearest-neighbour A and B atoms on a horizontal row. One can easily check that no spin configuration minimises all pair contributions to the energy of any square *plaquette*.

Periodic boundary conditions are imposed along the two directions. The system has N spins, N'' columns and $N' = N/N''$ sites per column or lines.

This model is *fully frustrated* since all plaquettes are. However, contrary to the fully frustrated model we have already discussed the absolute values of the coupling constants are not the same. The condition $0 < J_{AB} < |J_{BB}| < J_{AA}$ will be required from the exchanges.

Exercise 3.12 Compare the energy of all possible spin configurations on a square plaquette.

Due to the hierarchy in the absolute values of the coupling constants, ferromagnetic and anti-ferromagnetic order are favoured along the A and B columns, respectively. There are two possibilities for each. In contrast, no special order in the horizontal direction will be selected at $T = 0$. Indeed, if one looks at a single plaquette, one of the two horizontal links will be necessarily broken, but which one it is it does not matter.

The number of configurations that satisfy these requirements is $\Omega_0 = 2^{N''}$, each column has two choices for its FM (A) or AF (B) order, and the zero-point entropy ($k_B = 1$)

$$S_0 = \ln \Omega_0 = N'' \ln 2 \quad (3.49)$$

is proportional to the number of columns and therefore sub-extensive (as $N''/N = 1/N' \rightarrow 0$ in the thermodynamic $N' \rightarrow \infty$ limit; for example, for a square lattice $N' = N'' = L$

and $N = L^2$). The average magnetisation and staggered magnetisation vanish in the thermodynamic limit, as one can easily see from the typical ground state configuration in Fig. 3.13-left. The ground state (equilibrium at $T = 0$) is therefore globally disordered.

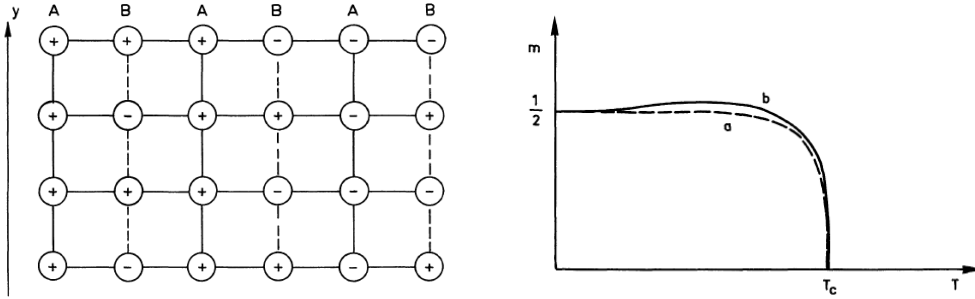


Figure 3.13: Left: The domino model and one of its ground states. Ferromagnetic bonds are full lines, antiferromagnetic bonds are dashed lines. Right: the magnetisation as a function of temperature. From [33].

The free-energy density can be computed with the *transfer matrix* method [35, 36], and it has a singularity at a critical temperature T_c given by

$$\sinh(2\beta_c |J_{AA} + J_{BB}|) \sinh(4\beta_c J_{AB}) = 1. \quad (3.50)$$

Above T_c the system is disordered and the equilibrium phase is paramagnetic. The low- $T > 0$ phase can be analysed from this exact solution or it can be characterised with a low temperature *decimation*. Basically, an effective model,

$$H_{J'}^{\text{eff}}[\{s_i^A\}] = \sum_{\langle ij \rangle} J'_{ij} s_i^A s_j^A \quad (3.51)$$

is obtained by summing over the spins in the B columns, s_i^B ,

$$Z = \sum_{\{s_i^A\}, \{s_i^B\}} e^{-\beta H_J[\{s_i^A, s_i^B\}]} \approx \sum_{\{s_i^A\}} e^{-\beta H_{J'}^{\text{eff}}[\{s_i^A\}]} = Z_{\text{eff}} \quad (3.52)$$

This calculation is not done exactly, but it is approximated by considering only the very low energy states. More precisely, given a column B sandwiched between two columns A, the two possible ground state orientations of the A columns are considered (parallel, FM or anti-parallel, AF) and the very low excitations in the B columns are summed over in the two cases. The ratio Z_{FM}/Z_{AF} is then compared to Z_{eff} for a $H_{J'}^{\text{eff}}$ with effective horizontal couplings. The new coupling strengths J'_{ij} are expressed in terms of the original ones and they are positive in both horizontal and vertical direction when

$$0 < J_{AB} < |J_{BB}| \ll J_{AA}. \quad (3.53)$$

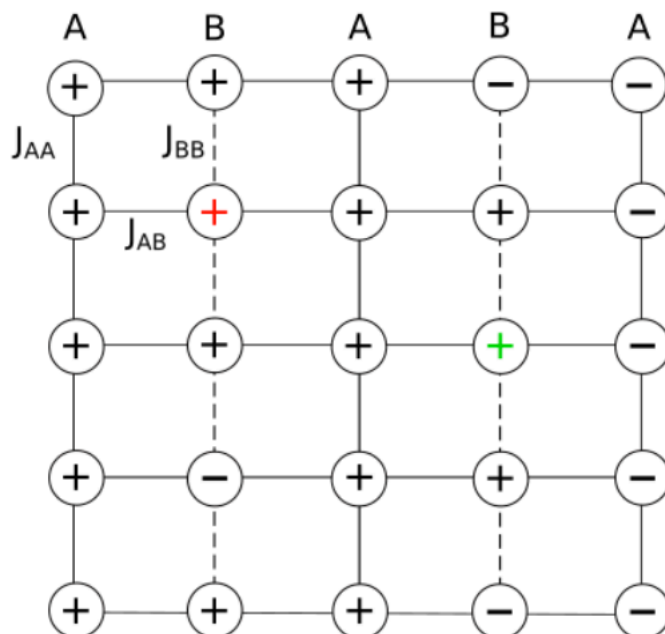


Figure 3.14: Two excitations in the domino model. Figure taken from H. Bacry's ENS stage report 2019.

Therefore, the system of A spins orders ferromagnetically at low temperatures, with $m_A \rightarrow 1$ for $T \rightarrow 0$. On the other hand the B spins have vanishing (ferromagnetic or staggered) magnetisation, $m_B = 0$, for $T \rightarrow 0$. In conclusion, $m = (m_A + m_B)/2 \rightarrow 1/2$ for $T \rightarrow 0$, contrary to $m = 0$ at $T = 0$.

Order by disorder is graphically represented as follows. At $T = 0$ the *manifold* of ground states in phase space has volume $\Omega_0 = 2^{N''}$. Among all these ground states there are two states with global ferromagnetic up or down order on the A columns. These two very special states are selected at $T = \epsilon$ by the entropic contribution to the free-energy.

The phenomenon of order by disorder in frustrated magnetic systems is not restrained to thermal fluctuations. Quantum, and even quenched noise may sometimes increase ordering in systems where energetics ensure a nontrivially degenerate classical disordered ground state.

Frustration \mapsto order by disorder

3.7 Discussion

Free-energy landscapes

Models with frustrated interactions often have complicated energy landscapes (over the large dimensional configuration space) and, more generally, free-energy landscapes as functions of the relevant order parameters that can be N . Sketches of these landscapes are often drawn in one dimension while, in reality, they are high dimensional. Finding the ground states, or at least the low lying minima, as well as the optimal paths over low lying saddle points, is still quite a challenge for simulations.

A theoretical approach to the physics of real glasses is based on the concept of frustration, which in this context describes an incompatibility between the extension of the locally preferred order in a liquid and tiling of the whole space. The real glass problem concerns the understanding of the behaviour of an ensemble of, say, particles in interaction which have been cooled fast enough to avoid nucleation (via a first order phase transition) into a stable crystal.

The ground state of four identical particles interacting via an isotropic potential is a perfect tetrahedron with the particles sitting at the vertices. However, it is not possible to fill space with such tetrahedra, see Fig. 3.15. The atom near the gap is frustrated because it cannot simultaneously sit in the minima provided by the pair potentials of its near neighbours. This frustration implies that there is no regular lattice of perfect tetrahedra which fills ordinary three-dimensional space. Familiar close-packed regular lattices, like the fcc structure, contain octahedra as well as tetrahedra. The octahedra are necessary to obtain a global tessellation of space, even though they do not minimise the energy locally.

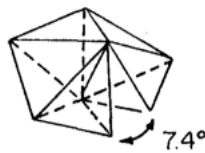


Figure 3.15: Frustration in a tetrahedral packing. Figure taken from [31].

This idea was put forward by D. Nelson [30] and its development over the years is discussed in [31] and [32].

Appendices

3.A Some useful formulæ

3.A.1 Fourier transform

Finite volume

We define the Fourier transform (FT) of a function $f(\vec{x})$ defined in a volume V as

$$\tilde{f}(\vec{k}) = \int_V d^d x f(\vec{x}) e^{-i\vec{k}\vec{x}} \quad (3.A.1)$$

This implies

$$f(\vec{x}) = \frac{1}{V} \sum_{\vec{k}} \tilde{f}(\vec{k}) e^{i\vec{k}\vec{x}} \quad (3.A.2)$$

where the sum runs over all \vec{k} with components k_i satisfying $k_i = 2m\pi/L$ with m an integer and L the linear size of the volume V .

Infinite volume

In the large V limit these equations become

$$\tilde{f}(\vec{k}) = \int_V d^d x f(\vec{x}) e^{-i\vec{k}\vec{x}} \quad (3.A.3)$$

$$f(\vec{x}) = \int_V \frac{d^d k}{(2\pi)^d} f(\vec{k}) e^{i\vec{k}\vec{x}} \quad (3.A.4)$$

On a lattice

Take now a function $f_{\vec{x}}$ defined on a lattice. Its Fourier transform is

$$\tilde{f}(\vec{k}) = \sum_{\vec{x}} f_{\vec{x}} e^{-i\vec{k}\vec{x}} \quad (3.A.5)$$

with the inverse

$$f_{\vec{x}} = \int \frac{d^d k}{2\pi} f(\vec{k}) e^{i\vec{k}\vec{x}} \quad (3.A.6)$$

and $\int d^d k / (2\pi)^d = \prod_{i=1}^d \int_{-\pi}^{\pi} dk_i / (2\pi) \cdots \int_{-\pi}^{\pi} dk_d / (2\pi)$ with these integrals running over the *first Brillouin zone* in reciprocal space.

Time domain

The convention for the Fourier transform is the time-domains is

$$f(\tau) = \int_{-\infty}^{\infty} \frac{d\omega}{2\pi} e^{-i\omega\tau} f(\omega) , \quad (3.A.7)$$

$$f(\omega) = \int_{-\infty}^{\infty} d\tau e^{+i\omega\tau} f(\tau) . \quad (3.A.8)$$

Properties

The Fourier transform of a real function $f(\vec{x})$ satisfies $\tilde{f}^*(\vec{k}) = \tilde{f}(-\vec{k})$.
The Fourier transform of the theta function reads

$$\theta(\omega) = i\text{vp}\frac{1}{\omega} + \pi\delta(\omega) . \quad (3.A.9)$$

The convolution is

$$[f \cdot g](\omega) = f \otimes g(\omega) \equiv \int \frac{d\omega'}{2\pi} f(\omega')g(\omega - \omega') . \quad (3.A.10)$$

3.A.2 Stirling

Stirling formula for the factorial of a large number reads:

$$\ln N! \sim N \ln N - \ln N , \quad \text{for } N \gg 1 . \quad (3.A.1)$$

3.A.3 Moments

Introducing a source h that couples linearly to a random variable x one easily computes all moments of its distribution $p(x)$. Indeed,

$$\langle x^k \rangle = \frac{\partial^k}{\partial h^k} \int dx p(x) e^{hx} \Big|_{h=0} . \quad (3.A.1)$$

3.A.4 Gaussian integrals

The Gaussian integral is

$$I_1 \equiv \int_{-\infty}^{\infty} \frac{dx}{\sqrt{2\pi\sigma^2}} e^{-\frac{(x-\mu)^2}{2\sigma^2}} = 1 . \quad (3.A.1)$$

It is the normalization condition of the Gaussian probability density written in the *normal form*. One has

$$\begin{aligned} \int_{-\infty}^{\infty} \frac{dx}{\sqrt{2\pi\sigma^2}} e^{-\frac{(x-\mu)^2}{2\sigma^2}} x &= \mu , \\ \int_{-\infty}^{\infty} \frac{dx}{\sqrt{2\pi\sigma^2}} e^{-\frac{(x-\mu)^2}{2\sigma^2}} x^2 &= \sigma^2 . \end{aligned} \quad (3.A.2)$$

From (3.A.1) one has

$$\int_{-\infty}^{\infty} \frac{dx}{\sqrt{2\pi\sigma^2}} e^{-\frac{x^2}{2\sigma^2} + \frac{\mu x}{\sigma^2}} = e^{\frac{\sigma^2 \mu^2}{2}}. \quad (3.A.3)$$

The generalization to N variables

$$I_N \equiv \int_{-\infty}^{\infty} \prod_{i=1}^N dx_i e^{-\frac{1}{2} \vec{x}^t A \vec{x} + \vec{x}^t \vec{\mu}} \quad (3.A.4)$$

with

$$\vec{x} = \begin{pmatrix} x_1 \\ x_2 \\ \dots \\ x_N \end{pmatrix}, \quad \vec{\mu} = \begin{pmatrix} \mu_1 \\ \mu_2 \\ \dots \\ \mu_N \end{pmatrix}, \quad A = \begin{pmatrix} A_{11} & \dots & A_{1N} \\ A_{21} & \dots & A_{2N} \\ \dots & \dots & \dots \\ A_{N1} & \dots & A_{NN} \end{pmatrix},$$

and

$$-\frac{1}{2} \vec{x}^t A \vec{x} + \vec{x}^t \vec{\mu} \quad (3.A.5)$$

is the most generic quadratic form. Note that A plays here the role σ^{-2} in the single variable case. One can keep the symmetric part $(A + A^t)/2$ of the matrix A only since the antisymmetric part $(A - A^t)/2$ yields a vanishing contribution once multiplied by the vectors \vec{x} and its transposed. Focusing now on a symmetric matrix, $A^t = A$, that we still call A we can ensure that it is diagonalizable and all its eigenvalues are positive definite, $\lambda_i > 0$. One can then define $A^{1/2}$ as the matrix such that $A^{1/2} A^{1/2} = A$ and its eigenvalues are the square root of the ones of A . Writing $\vec{x}^t A \vec{x} = (\vec{x}^t A^{1/2})(A^{1/2} \vec{x}) = \vec{y}^t \vec{y}$, the integral I_N in (3.A.4) becomes

$$I_N = \int_{-\infty}^{\infty} \prod_{i=1}^N dy_i J e^{-\frac{1}{2} \vec{y}^t \vec{y} + \vec{y}^t (A^{-1/2} \vec{\mu})} \quad (3.A.6)$$

where $J = \det(A^{1/2})^{-1} = (\det A)^{-1/2}$ is the Jacobian of the change of variables. Calling $\vec{\mu}'$ the last factor one has the product of N integrals of the type I_1 ; thus

$$I_N = (2\pi)^{N/2} (\det A)^{-1/2} e^{\frac{1}{2} \vec{\mu}'^t A^{-1} \vec{\mu}} \quad (3.A.7)$$

Finally, the functional Gaussian integral is the continuum limit of the N -dimensional Gaussian integral

$$\vec{x} \equiv (x_1, \dots, x_N) \rightarrow \phi(\vec{x}) \quad (3.A.8)$$

and

$$I = \int \mathcal{D}\phi e^{-\frac{1}{2} \int d^d x d^d y \phi(\vec{x}) A(\vec{x}, \vec{y}) \phi(\vec{y}) + \int d^d x \phi(\vec{x}) \mu(\vec{x})}. \quad (3.A.9)$$

The sum runs over all functions $\phi(\vec{x})$ with the spatial point \vec{x} living in d dimensions. The first and the second term in the exponential are quadratic and linear in the field, respectively. In analogy with the I_N case the result of the *path integral* is

$$I \propto e^{\frac{1}{2} \int d^d x d^d y \mu(\vec{x}) A^{-1}(\vec{x}, \vec{y}) \mu(\vec{y})} \quad (3.A.10)$$

where we ignore the proportionality constant. Indeed, this one depends on the definition of the path-integral measure $\mathcal{D}\phi$. Usually, the actual value of this constant is not important since it does not depend on the relevant parameters of the theory. The inverse A^{-1} is defined by

$$\int d^d y A^{-1}(\vec{x}, \vec{y}) A(\vec{y}, \vec{z}) = \delta(\vec{x} - \vec{z}) . \quad (3.A.11)$$

3.B Wick's theorem

Take a Gaussian variable x with mean $\langle x \rangle = \mu$ and variance $\sigma^2 = \langle x^2 \rangle - \langle x \rangle^2$. Its pdf is

$$p(x) = (2\pi\sigma^2)^{-1/2} e^{-(x-\mu)^2/(2\sigma^2)} . \quad (3.B.1)$$

All moments $\langle x^k \rangle$ can be computed with (3.A.1). One finds

$$\langle e^{hx} \rangle = e^{\frac{h^2\sigma^2}{2} + h\mu} \quad (3.B.2)$$

and then

$$\langle x^k \rangle = \left. \frac{\partial^k}{\partial h^k} e^{\frac{h^2\sigma^2}{2} + h\mu} \right|_{h=0} \quad (3.B.3)$$

from where

$$\begin{aligned} \langle x \rangle &= \mu , & \langle x^2 \rangle &= \sigma^2 + \mu^2 , \\ \langle x^3 \rangle &= 3\sigma^2\mu + \mu^3 , & \langle x^4 \rangle &= 3\sigma^4 + 6\sigma^2\mu^2 + \mu^4 \end{aligned}$$

etc. One recognizes the structure of Wick's theorem: given k factors x one organises them in pairs leaving the averages μ aside. The simplest way of seeing Wick's theorem in action is by drawing examples.

The generalization to N Gaussian variables is immediate. Equation (3.B.2) becomes

$$\langle e^{\vec{h}\vec{x}} \rangle = e^{\frac{1}{2}\vec{h}A^{-1}\vec{h} + \vec{h}\vec{\mu}} \quad (3.B.4)$$

and the generalization of (3.B.3) leads to

$$\langle x_i \rangle = \mu_i , \quad \langle x_i x_j \rangle = A^{-1}_{ij} + \mu_i \mu_j , \quad (3.B.5)$$

etc. In other words, wherever there is σ^2 in the single variable case we replace it by A^{-1}_{ij} with the corresponding indices.

The generalization to a field theory necessitates the introduction of functional derivatives that we describe below. For completeness we present the result for a scalar field in d dimensions here

$$\langle \phi(\vec{x}) \rangle = \mu(\vec{x}) , \quad \langle \phi(\vec{x})\phi(\vec{y}) \rangle = A^{-1}(\vec{x}, \vec{y}) + \mu(\vec{x})\mu(\vec{y}) , \quad (3.B.6)$$

etc.

3.C Functional analysis

A functional $F[h]$ is a function of a function $h : \vec{x} \rightarrow h(\vec{x})$. The variation of a functional F when one changes the function h by an infinitesimal amount allows one to define the functional derivative. More precisely, one defines $\delta F \equiv F[h + \delta h] - F[h]$ and one tries to write this as $\delta F = \int d^d x \alpha(\vec{x}) \delta h(\vec{x}) + \frac{1}{2} \int d^d x d^d y \beta(\vec{x}, \vec{y}) \delta h(\vec{x}) \delta h(\vec{y}) + \dots$ and one defines the functional derivative of F with respect to h evaluated at the spatial point \vec{x} as

$$\frac{\delta F}{\delta h(\vec{x})} = \alpha(\vec{x}), \quad \frac{\delta^2 F}{\delta h(\vec{x}) \delta h(\vec{y})} = \beta(\vec{x}, \vec{y}) \quad (3.C.1)$$

etc. All usual properties of partial derivatives apply.

3.D The saddle-point method

Imagine one has to compute the following integral

$$I \equiv \int_a^b dx e^{-Nf(x)}, \quad (3.D.1)$$

with $f(x)$ a positive definite function in the interval $[a, b]$, in the limit $N \rightarrow \infty$. It is clear that due to the rapid exponential decay of the integrand, the integral will be dominated by the minimum of the function f in the interval. Assuming there is only one absolute minimum, x_0 , one then Taylor expands $f(x)$ upto second order

$$f(x) \sim f(x_0) + \frac{1}{2} f''(x_0) (x - x_0)^2 \quad (3.D.2)$$

and obtains

$$I \sim e^{-Nf(x_0)} \int_a^b dx e^{-N \frac{1}{2} f''(x_0) (x - x_0)^2} = e^{-Nf(x_0)} [N f''(x_0)]^{-1/2} \int_{y_a}^{y_b} dy e^{-\frac{1}{2} (y - y_0)^2}, \quad (3.D.3)$$

with $y_0 \equiv \sqrt{N f''(x_0)} x_0$ and similarly for y_a and y_b . The Gaussian integral is just an error function that one can find in Tables.

This argument can be extended to multidimensional integrals, cases in which there is no absolute minimum within the integration interval, cases in which the function f is not positive definite, etc.

References

- [1] G. Toulouse, *Theory of frustration effects in spin-glasses*, Comm. Phys. **2**, 115 (1977).
- [2] J. F. Sadoc and R. Mosseri, *Geometrical Frustration*, (Cambridge Univ. Press, 1999), reedited 2007.
- [3] R. Moessner and A. P. Ramírez, *Geometrical Frustration*, Physics Today 2006.
- [4] *Frustrated spin systems*, H. T. Diep ed. (World Scientific, 2004).
- [5] F. Mila, *Frustrated Spin Systems*, in *Many-Body Physics: From Kondo to Hubbard*, Autumn School on Correlated Electrons, E. Pavarini, E. Koch, and P. Coleman eds., 2015.
- [6] D. C. Mattis, *Solvable Spin Systems with Random Interactions*, Phys. Lett. A **56**, 421 (1976).
- [7] J. J. Hopfield, *Neural networks and physical systems with emergent collective computational abilities*, Proc. Natl. Acad. Sci. USA **79**, 2554 (1982).
- [8] D. J. Amit, H. Gutfreund, H. Sompolinsky, *Statistical Mechanics of Neural Networks near Saturation*, Ann. Phys. **173**, 30 (1987).
- [9] L. Pauling, *The structure and entropy of ice and other crystals with some randomness of atomic arrangements*, J. Chem. Phys. **57**, 2680 (1935).
- [10] R. M. F. Houtappel, *Order-disorder in hexagonal lattices*, Physica **16**, 425 (1950).
- [11] G. H. Wannier, *Antiferromagnetism. The triangular Ising net*, Phys. Rev. **79**, 357 (1950).
- [12] L. Onsager, *Crystal statistics. I. A two-dimensional model with an order-disorder transition*, Phys. Rev. **65**, 117 (1944).
- [13] B. D. Metcalf and C. P. Yang, *Degeneracy of antiferromagnetic Ising lattices at critical magnetic field and zero temperature*, Phys. Rev. B **18**, 2304 (1978).
- [14] J. Stephenson, *Ising model spin correlations on triangular lattice*, J. Math. Phys. **5**, 1009 (1964).
- [15] H. W. J. Blöte and H. J. Hilhorst, *Roughening transitions and the zero-temperature triangular Ising antiferromagnet*, J. Phys. A: Math. Gen. **15**, L631 (1982).
- [16] B. Nienhuis, H. W. J. Blöte and H. J. Hilhorst, *Triangular SOS models and cubic-crystal shapes*, J. Phys. A: Math. Gen. **17** (1984) 3559.

- [17] J. T. Chalker, *Spin liquids and frustrated magnetism*, in *Topological aspects of condensed matter physics*, Les Houches Summer School 2014, C. Chamon, M. Görbig, R. Moessner and L. F. Cugliandolo eds. (Oxford University Press).
- [18] M. Kardar, *Crossover to equivalent-neighbor multicritical behavior in arbitrary dimensions*, Phys. Rev. Lett. **28**, 244 (1983).
- [19] F. Bouchet, S. Gupta, and D. Mukamel, *Thermodynamics and dynamics of systems with long-range interactions*, arXiv:1001.1479 (2010).
- [20] J. Villain, *Spin glass with non-random interactions*, J. Phys. C: C: Solid State Phys. **10**, 1717 (1977).
- [21] C. Rottman and M. Wortis, *Statistical mechanics of equilibrium crystal shapes - interfacial phase diagrams and phase transitions*, Phys. Rep. **103**, 59 (1984).
- [22] J. F. Nagle, J. Math. Phys. **7**, 1484 (1966).
- [23] E. H. Lieb, *Exact solution of problem of entropy of 2-dimensional ice*, Phys. Rev. Lett. **18**, 692 (1967), *Exact solution of F model of an antiferroelectric*, Phys. Rev. Lett. **18**, 1046 (1967), *Exact solution of 2-dimensional Slater KDP model of a ferroelectric*, Phys. Rev. Lett. **19**, 108 (1967).
- [24] R. J. Baxter, *Exactly Solved Models in Statistical Mechanics* (Dover, New York, 1982).
- [25] W. F. Giauque and J. W. Stout, *The entropy of water and the third law of thermodynamics - The heat capacity of ice from 15 to 273 degrees K*, J. Am. Chem. Soc. **58**, 1144 (1936). A. P. Ramírez, A. Hayashi, R. J. Cava, R. S. Siddharthan and B. S. Shastry, *Zero-point entropy in 'spin ice'*, Nature **399**, 333 (1999).
- [26] L. F. Cugliandolo, G. Gonnella and A. Pelizzola, *Six-vertex model with domain wall boundary conditions in the Bethe-Peierls approximation*, J. Stat. Mech. P06008 (2015).
- [27] M. E. Fisher, *Statistical mechanics of dimers on a plane lattice*, Phys. Rev. **124**, 1664 (1961).
- [28] M. Grousson, G. Tarjus, and P. Viot, *Phase diagram of an Ising model with long-range frustrating interactions: A theoretical analysis*, Phys. Rev. E **62**, 7781 (2000).
- [29] M. Antonietti and C. Göltner, Angew. Chem. Int. Ed. Engl. **36**, 910 (1997)
- [30] D. R. Nelson, *Order, frustration and defects in liquids and glasses*, Phys. Rev. B **28**, 5515 (1983).
- [31] D. R. Nelson, *The structure and statistical mechanics of glass*, Lecture Notes in Physics **216**, 13 (1985).

-
- [32] G. Tarjus, S. A. Kivelson, Z. Nussinov and P. Viot, *The frustration-based approach of supercooled liquids and the glass transition: a review and critical assessment*, J. Phys.: Condens. Matter **17**, R1143 (2005).
- [33] J. Villain, R. Bidaux, J.-P. Carton, and R. Conte, *Order as an effect of disorder*, J. Physique **41**, 1263 (1980).
- [34] E. F. Shender and P. W. C. Holdsworth, *Order by disorder and frustration in magnetic systems*, in *Fluctuations and order*, M. Millonas ed. (Springer, 1996).
- [35] H. A. Kramers and G. H. Wannier, *Statistics of the two-dimensional ferromagnet Part I*, Phys. Rev. **60**, 252 (1941). *Statistics of the two-dimensional ferromagnet Part II*, Phys. Rev. **60**, 263 (1941).
- [36] L. Onsager, *Crystal statistics I A two-dimensional model with an order-disorder transition*, Phys. Rev. **65**, 117 (1944).